CORE
Metadata, citation and similar papers at core.ac.uk
Provided by Qucosa - Publikationsserver der Universität Leipzig

diffusion-fundamentals.org
The Open-Access Journal for the Basic Principles of Diffusion Theory, Experiment and Application

A Nuclear Magnetic Resonance Pulsed Field Gradient Study of Self-Diffusion of Water in Hydrated Cement Pastes

V. V. Rodin, P. J. McDonald, S. Zamani

Department of Physics, University of Surrey, Guildford, Surrey GU2 7XH, UK

Corresponding author: Victor Rodin, E-mail: v.rodin@surrey.ac.uk

Abstract

The results of one- and two-dimensional ^{1}H nuclear magnetic resonance (NMR) pulsed field gradient (PFG) diffusometry studies of water in white cement paste with a water-to-cement ratio 0.4 and aged from 1 day to 1 year are reported. The study shows that the NMR-PFG method is primarily sensitive to the capillary porosity. Data is fit on the basis of a log-normal pore size distribution with pore size dependent relaxation times. The volume mean capillary pore size is 4.2 μm in mature paste, similar to 1 week suggesting that hydrates and gel porosity do not form in the capillary porosity once the latter has been substantially created. No evidence is found of capillary pore anisotropy in cement paste.

Keywords

Cement, diffusion, porosity, NMR, PFG.

1. Introduction

A detailed understanding of microstructure, pore-water interactions and water diffusion in cement, the binder phase of concrete, remains elusive even though concrete is used globally in vast quantities. This is because cement is highly heterogeneous and morphologically complex on multiple length scales. Nuclear magnetic resonance (NMR) pulsed field gradient (PFG) diffusometry [1,2] is a well established method for measuring the self diffusion coefficient, D, of small molecules in liquids. The time dependence of the apparent diffusion coefficient D_{app} for liquids in porous media – restricted diffusion - can yield information about the confining microstructure. The method has been applied previously to cements [3,4]. However, cements pose multiple challenges. First, large magnetic field gradients due to inhomogeneity of the sample magnetic susceptibility can swamp the applied field gradients making quantitative measurement difficult. Second, cement paste has small pores, so mean free paths are very limited. Third, NMR relaxation times (spin-spin and spin-lattice) are very short, limiting the maximum length, δ, and separation, Δ, of the gradient pulses that can be applied. For these reasons, the method is primarily sensitive to capillary pore water.

© 2013, Victor Rodin

We report one- and two-dimensional ^{1}H PFG studies of water in white cement paste. Pastes are cured for periods of one to fourteen days and one year. We have adapted a well known expression for restricted diffusion in a Gaussian distribution of pore sizes [5] to the case of a log-normal distribution for which the relaxation times T_1 and T_2 are pore size dependent. The pore sizes discovered are micron in size and correspond to the capillary network. It is believed that smaller gel and inter calcium silicate hydrate (C-S-H) layer spaces in cement are broadly planar [6,7]. Therefore, we have looked for evidence of anisotropy in the nascent gel and capillary pore network of young samples using two-dimensional NMR PFG methods. No anisotropy was seen.

2. Materials and methods

2.1. Materials

Low C_3A white cement was obtained from the Nanocem consortium (www.nanocem.org). Cement was mixed into paste with a water to cement ratio of 0.4 by mass using methods established by Nanocem [8]. Samples were cast in 8 mm diameter and 7 mm deep cylindrical moulds and, once set (15 hrs), cured under saturated $Ca(OH)_2$ solution. Hence, sufficient capillary water remained to measure even after 1 year. Prior to NMR-analysis, samples were dabbed dry and placed in sealed NMR tubes with glass rods to take up the free volume.

2.2. Methods

NMR measurements were made using a 400 MHz Chemagnetics Infinity spectrometer equipped with a 10 mm Fraunhofer Institute ^{1}H probe and an 89 mm bore Magnex superconducting magnet. The 90° pulse width was 10 μs and the spectrometer dead time 6-8 μs. NMR PFG studies have been realised in one- and two-dimensions. In one-dimension, the spin-echo (SE) pulse sequence [9] was used with echo times ($2\tau_2$) ranging from 12 to 28 ms and gradient pulses of duration δ = 2 ms and maximum amplitude G_{max} = 1.5 T/m and with encoding time $\Delta = \tau_2$. The three pulse stimulated-echo (STE) sequence [10] was also used with storage times τ_1 and encoding times $\Delta = \tau_1 + \tau_2$ up to 50 ms. Sequences are available to negate the deleterious effects of internal magnetic field susceptibility gradients. A popular choice, as discussed by [11], is that due to Cotts *et al.* [12]. The Cotts sequence introduces bipolar gradient pairs separated by additional 180° pulses in place of each gradient pulse of the STE sequence. We implemented the Cotts variant shown in Figure 4a of reference [12] using a bipolar pair of 1 ms gradient pulses in place of each 2 ms pulse. Up to 1024 averages with a repetition time of 1 s were recorded per echo spectrum. In two dimensions, diffusion-diffusion correlation experiments (DDCOSY) [13] comprising of two spin echoes created by two pairs of pulsed field gradient were carried out with encoding times of 6 ms and gradients in x and y-directions. T_2 distributions in pastes were measured using Carr Purcell Meiboom Gill experiments with a pulse gap interval of 25 μs and 200 echoes. Echo decays were inverted using the Inverse Laplace Transform algorithm due to Venkataramanan *et al* [14]. Other analysis was conducted using in-house MatLab® codes.

3. Theory and models

3.1. PFG SE and PFG STE

The NMR echo intensity recorded in the presence of a pair of field gradient pulses of strength G, duration δ and separation Δ is smaller than the echo in the absence of the gradients due to diffusive attenuation. For small molecules diffusing in bulk liquids the additional echo attenuation $I(G)/I(0)$ is given by:

© 2013, Victor Rodin

$$\frac{I(G)}{I(0)} = \exp\left(-q^2(\Delta - \delta/3)D\right) \tag{1}$$

where $q = \gamma G\delta$ and γ is the (^{1}H) nuclear magnetogyric ratio. The equivalent result for echo attenuation for the Cotts sequence is given as Eq. (5) in [12]. It includes a factor for the applied gradient similar to Eq. (1), a corresponding term for the background gradient and a cross term. Note the notation used throughout this work, which follows [9] differs from that adopted in [12], most notably in the definition of Δ.

There is much further literature on the form of the echo attenuation in the case of molecules in porous media. For small pores, size r, in the long time limit model ($\Delta >> r^2/D$) it has been shown by Callaghan *et al*. [5] that the echo attenuation is well approximated by:

$$\frac{I(G)}{I(0)} = \exp\left(-\beta^2 r^2\right) \tag{2}$$

where $\beta^2 = q^2/5$. The same authors go on to present a development of this result applicable to a Gaussian volume distribution of spherical pore sizes:

$$\frac{I(\delta, G, r_0, \sigma)}{I(0)} = \frac{1}{\sqrt{1+2\sigma^2\beta^2}} \exp\left(-\frac{\beta^2 r_0{}^2}{1+2\sigma^2\beta^2}\right) \tag{3}$$

where r_0 is average pore size and σ is standard deviation. However in cement pastes the nuclear spin relaxation times are strongly pore size dependent. It has previously been shown that, to a good approximation, $T_1 = \alpha T_2$ and that $T_2 = r/3\lambda$ [15-17] (assuming spherical pores) where λ is the surface relaxivity and α is a constant. Hence, we prefer to explicitly write the integral formulae for a distribution of sizes:

$$I(G,r) = \int_r I_0(r) \exp\left(-\beta^2 r^2\right) \exp\left(-6\lambda\tau_2/r\right) \exp\left(-3\lambda\tau_1/\alpha r\right) dr \tag{4}$$

where τ_1 is zero and τ_2 is the pulse gap in the SE experiment and τ_1 and τ_2 are the separation of second and third and first and second RF pulses respectively of the STE pulse sequence, and $I_0(r)$ is proportional to the distribution of pore volumes. The signal attenuation can be calculated by numerical integration and a global fit to data acquired as a function of $\Delta = \tau_1 + \tau_2$, τ_2 and G. Experimentally, in similar pastes at 20 MHz, $\alpha = 4$ and $\lambda = 0.0037$ nm/μs. At 400 MHz, α is about ≈ 9 times larger [18], while λ is expected to be comparable [16].

3.2. Diffusion-diffusion correlation in study of local order

Full details of the DDCOSY experiment analysis are to be found in the literature [1,13]. A 2D Inverse Laplace Transform of the resultant data set,

$$\frac{I(q_1^2, q_2^2)}{I_0} = \exp(-q_1^2 D_1 \Delta_1) \exp(-q_2^2 D_2 \Delta_2) \tag{5}$$

yields a spectrum that reveals anisotropy of the diffusion tensor. The powder average for a system with locally axially symmetric diffusion tensor, see references, is especially tractable and commonly studied.

© 2013, Victor Rodin

4. Results and analysis

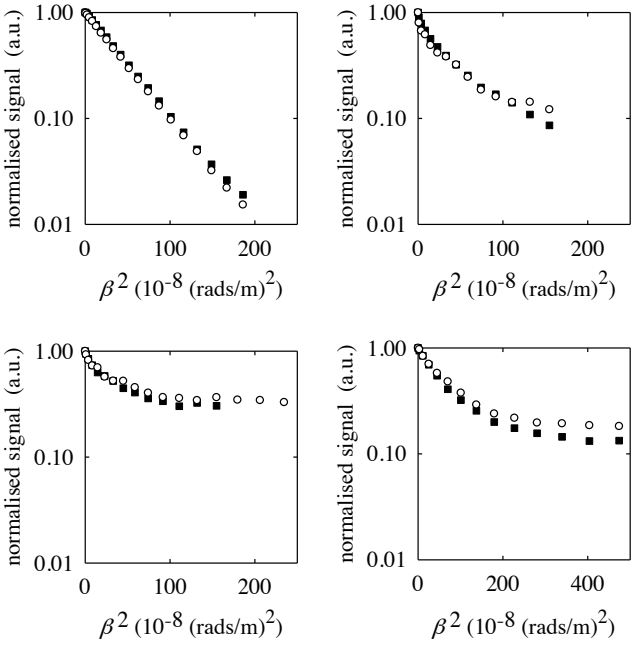

Fig. 1. Comparison of gradient attenuation curves for the Cotts (open circles) and STE (solid squares) sequences for water (top left) and cement paste after 2½ (top right), 4 (bottom left) and 9 (bottom right) days hydration. Left: Δ = 30 ms; right: Δ = 18 ms.

4.1. Internal gradients: Comparison of the Cotts and STE sequences.

The use of the Cotts sequence was compared to STE. Figure 1 shows the direct comparison for water, and for a cement paste after 2.5, 4 and 9 days hydration variably for Δ = 18 or 30 ms. It is seen that agreement between the two data sets is excellent in the case of water, as expected. It is also surprisingly good in the case of white cement. This suggests that background gradients due to heterogeneity of the magnet susceptibility is having substantially less effect than might have been expected. One reason that the internal gradients may not be as severe as expected is that iron (the leading, but nonetheless small, source of paramagnetic impurity in white cement) does not distribute uniformly throughout the paste but rather aggregates in nano-crystalline AFm or hydrogarnet phases [19]. Given this finding, we do not use the Cotts sequence, nor consider background gradients further in this work. This is for two reasons. First the presence of the cross term in the Cotts echo attenuation formulae, and the fact that the background gradient is probably pore size dependent, significantly complicate the calculation of pore size distributions using Eqs (3) and (4). Second, the requirement to introduce additional gradient switching delays into the pulse sequence that increase signal relaxation attenuation, and other signal loss mechanisms, as discussed by Wu *et al*. [20], reduce the signal-to-noise ratio of the experiment when this is already a severe limitation.

4.2. Diffusion during early hydration of cement paste

CPMG decays were measured as a function of hydration time for a cement paste. As reported elsewhere [21,22] they showed that from 1 day onwards, the overwhelming majority of the signal has T_2 relaxation times of the order of, or less than, 1 ms corresponding to bound water and water in nanometre sized pores. Only a very small fraction had substantially larger relaxation times corresponding to water in micron sized capillary pores. Nonetheless, it is this fraction that dominates the echo signal seen in PFG experiments.

© 2013, Victor Rodin

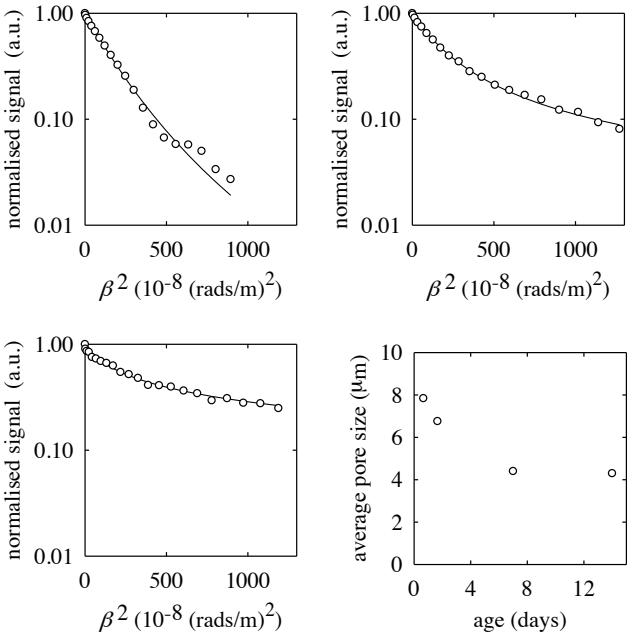

Fig. 2. PFG-SE attenuation curves for cement paste for hydration times of 15 hours (top left), 2 days (top right) and 14 days (bottom left). The experimental parameters are $\Delta = 6$ ms and $\delta = 2$ ms. Bottom right: the mean pore size evaluated from the attenuation curves according to Eq. (3).

During the early stages of hydration, the sample morphology is evolving too quickly to enable a full multi-parameter data set to be measured. Rather, measurements with sufficient signal-to-noise ratio can only be made for one value of Δ and δ (here 6 and 2 ms respectively) and for a series of values of G. Fig. 2 shows the results of such measurements for a sample after 15 hrs, 2 days and 14 days of hydration. It is seen that the log-echo decays are non-linear indicating restricted diffusion. Consequently, the data sets have been fit to Eq. (3). The resultant mean pore size as a function of hydration time is shown in Fig. 1 bottom right. It attains 4 μm by 1 week. The pore size distribution widths given by the data fits are comparable to the mean sizes suggesting a broad distribution but also reflecting the limitations of the model. The largest mean pore size calculated is 8 μm. Given the bulk diffusivity of water, 2.3×10^{-9} m^2/s [23] and the shortest $\Delta = 6$ ms, we calculate that we are just within the long time limit since $(6D\Delta)^{1/2} = 9$ μm > 8 μm in the worst case scenario.

4.3. Diffusion in mature paste

The average pore size is of the order of microns, but the fact that the T_2 relaxation is strongly pore size dependent, means that large pores are over-represented in the signal. In order to overcome this difficulty, a data set was acquired at $\delta = 2$ ms as a function of Δ ($6 \text{ ms} \le \Delta \le 50$ ms) and G ($0 \le G \le 1.2$ T/m) for a mature (1 year) paste. A global fit to the data was made using Eq. (4) with $\alpha = 35$ and fit parameters, r_0, σ and λ on the basis of a log-normal volume distribution of pore sizes so that:

$$I_0(r) \propto \frac{1}{\sigma r \sqrt{2\pi}} \exp\left(-\frac{\left(\ln(r/r_0)\right)^2}{2\sigma^2} \right) \tag{6}$$

where r_0 is the mean pore size and σ is dimensionless width parameter. The data and global best fit are shown in Fig. 3 (left). The fit parameters are $r_0 = 4.2$ μm, $\sigma = 0.51$ and $\lambda = 0.7$ nm/μs. It is noticeable that the size of capillary pores after one year is comparable to that after 1 week. The NMR evidence is therefore that the C-S-H and gel pore network does not fill the capillary porosity, once created, as the former grows. The analysis is insensitive to the chosen value of α and only weakly sensitive to λ, although the latter is significantly larger than expected. We note that fits are only marginally worse by eye by fixing

$\lambda = 0.0037$ nm/μs, see section 3.1, and allowing α to float. In this case $r_0 = 9.0$ μm, $\sigma = 0.37$ and $\alpha = 12$. However, now the resultant relaxation times in the biggest pores are unreasonably large. Single component fits to plots of ln($I(G=0)$) against $2\tau_2$ (SE data) or τ_1 at constant τ_2 (STE data), Fig. 3 (right) yield T_2 and T_1 values of 24 and 43 ms respectively. These times are less than predicted by scaling low frequency, nano-pore results (fixed λ) but are more than those for the first analysis. We attribute these discrepancies to over simplified application of the model of relaxation in large pores, and to residual diffusive attenuation effects in background gradients. T_2 decays in particular are more normally measured using echo trains with closely spaced echoes to alleviate the problem.

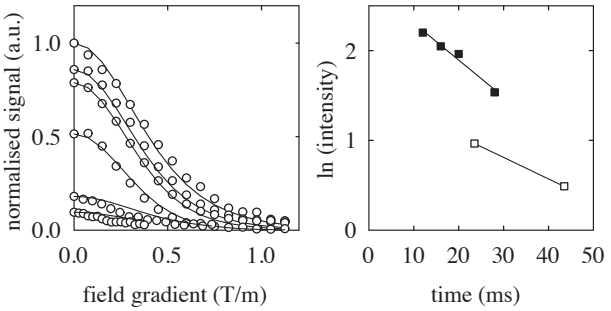

Fig. 3. (Left) Exemplar echo decay curves and global fitting for a year-old cement paste with initial water-to-cement ratio 0.4. The curves are for different values of $\Delta = \tau_2 + \tau_1$ (from top: 6; 8; 10; 14; 30 and 50 ms) and τ_2 (6, 8, 10, 14, 6.4 and 6.4 ms) all with $\delta = 2$ ms. (Right) Plot of ln(I ($G = 0$)) against $2\tau_2$ (SE: solid points) and τ_1, (STE: lower points). The trend lines have decay constants 24 and 43 ms respectively.

4.3. DDCOSY

In order to check that the DDCOSY experiment is working correctly, Fig. 4 (top) shows spectra recorded from bulk water and a sample of wet wood. The bulk water diffuses freely whereas water in the wood is confined within highly anisotropic cells, tens of microns in size. As expected only a single diagonal peak is seen in the case of bulk water whereas a more complex pattern is seen for wood. This pattern is consistent with simulations, not shown, for a powder average system using similar experimental parameters in which the local diffusion tensor is cylindrically symmetric with diffusion on-axis an order of magnitude smaller than orthogonal to the axis.

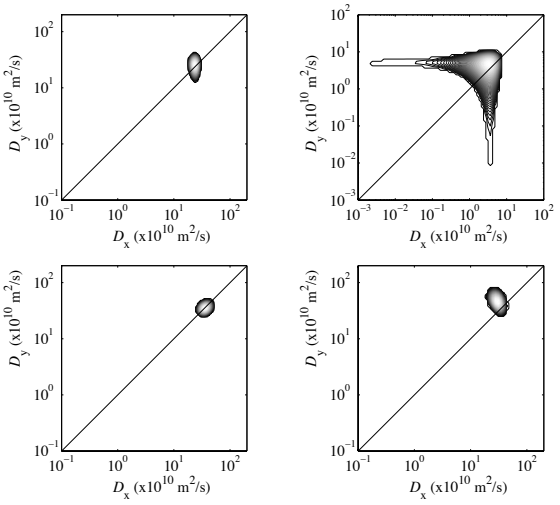

Fig. 4. Diffusion-diffusion correlation spectra for bulk water (top left), wood (top right) and cement paste at 1 day (bottom left) and 2 days bottom right. In each case the spectrum is derived from a 20 × 20 data set with $\delta_{1,2} = 1$ms, $\Delta_{1,2} = 6$ms. The maximum gradient strength is 1.2 T/m. Only the wood reveals a signature of an anisotropic diffusion tensor. The data bottom left was recorded at 3 °C in order to slow hydration of the cement. (Note that the axis scale varies across the plots).

Fig. 4 (bottom) shows DDCOSY spectra of cement samples after 1 and 2 days hydration. The data at 1 day was recorded at 3 °C in an attempt to slow the hydration kinetics and hence to allow more time for data acquisition with an unchanging sample. Both plots are similar to Fig. 4 (top left) and suggest water diffusion in young capillary pores is isotropic. There is no evidence for anisotropy in the pore shapes. This is consistent with micrograph evidence that typically shows anisotropy of small gel pores, but not the larger capillary pores [24,25].

© 2013, Victor Rodin

5. Conclusion

Pulsed field gradient experiments have revealed the typical pore size of capillary pores in cements. Once established after a few days hydration, they do not change significantly, they do not infill. The NMR analysis has been extended to allow for a log-normal distribution of sizes with spin relaxation rates inversely proportional to the pore size. Two dimensional correlation experiments have found no evidence for capillary pore anisotropy in cement. The effects of internal susceptibility gradients were shown to be surprisingly small.

Acknowledgments

The authors thank: Y.-Q. Song of Schlumberger-Doll Research for 2D Fast Laplace Inversion software; R. Derham, University of Surrey, for help with experiments; and the UK Engineering and Physical Sciences Research Council (grant no.: EP/H033343/1) for funding.

References

[1] P.T. Callagan, Translational Dynamics and Magnetic Resonance, Oxford University Press, 2011.
[2] R. Kimmich, NMR: Tomography, Diffusometry, Relaxometry, Springer, 2001.
[3] R. Blinc, M. Burgar, G. Lahajnar, M. Rozmarin, V. Rutar, I. Kocuvan, J. Ursic, J. Am. Ceram. Soc. 61 (1978) 35.
[4] N. Nestle, P. Galvosas, J. Kärger, Cem. Conc. Res. 37 (2007) 398.
[5] P.T. Callaghan, K.W. Jolley, R.S. Humphrey, J. Colloid Interface Sci. 93 (1983) 521.
[6] R.F. Feldman, P.J. Sereda, Engineering Journal 53 (1970) 53.
[7] A.J. Allen, J.J. Thomas, H.M. Jennings, Nat. Mater. 6 (2007) 311.
[8] P.J. McDonald, V. Rodin, A. Valori, Cem. Conc. Res. 40 (2010) 1656.
[9] E.O. Stejskal, J.E. Tanner, J. Chem. Phys. 42 (1965) 288.
[10] J.E. Tanner, J. Chem. Phys. 52 (1970) 2523.
[11] J.G. Seland, G.H. Sørland, K. Zick, B. Hafskjold, J. Magn. Reson. 146 (2000) 14.
[12] R.M. Cotts, M. Hoch, T. Sun, J.T. Markert, J. Magn. Reson. 83 (1989) 252.
[13] P.T. Callaghan, I. Furó, J. Chem. Phys. 120 (2004) 4032.
[14] L. Venkataramanan, Yi-Qiao Song, M.D. Hurlimann, IEEE Trans. Signal Process. 50 (2002) 1017.
[15] K.S. Mendelson, W.P. Halperin, J.-Y. Jehng, Y.-Q. Song, Magn. Reson. Imag. 12 (1994) 207.
[16] P.J. McDonald, J.P. Korb, J. Mitchell, L. Monteilhet, Phys. Rev. E 72 (2005) 011409.
[17] L. Monteilhet, J.P. Korb, J. Mitchell, P.J. McDonald, Phys. Rev. E 74 (2006) 061404.
[18] P.J. McDonald, J. Mitchell, M. Mulheron, P.S. Aptaker, J.P. Korb, L. Monteilhet, Cem. Conc. Res. 37 (2007) 303.
[19] B.Z. Dilnesa, "Fe-Containing Hydrates and Their Fate During Cement Hydration: Thermodynamic Data and Experimental Study", PhD thesis, EPFL, Switzerland, 2011.
[20] D.H. Wu, A.D. Chen, C.S. Johnson, J. Magn. Reson. A 115 (1995) 260.
[21] A.C.A. Muller, K.L. Scrivener, A.M. Gajewicz, P.J. McDonald, Microporous and Mesoporous Materials (2013).
[22] A.C.A. Muller, K.L. Scrivener, A.M. Gajewicz, P.J. McDonald, J. Phys. Chem. C 117 (2013) 403.
[23] K. Krynicki, C.D. Green, D.W. Sawyer, Faraday Discuss. Chem. Soc. 66 (1978) 199.
[24] I.G. Richardson, Cem. Conc. Res. 29 (1999) 1131.
[25] E. Gallucci, K. Scrivener, A. Groso, M. Stampanoni, G. Margaritondo, Cem. Conc. Res. 37 (2007) 360.

© 2013, Victor Rodin